Inverse Relationship between the Kinetic and Thermodynamic Stabilities of the Misdirected Ligand Complexes Δ/Λ-(δ/λ-1,1′-Biisoquinoline)bis(2,2′-bipyridine)metal(II) (metal = Ruthenium, Osmium)†

Michael T. Ashby

Contribution from the Department of Chemistry and Biochemistry, University of Oklahoma, Norman, Oklahoma 73019

Received October 31, 1994®

Abstract: Δ/Λ-(δ/λ-1,1′-biisoquinoline)bis(2,2′-bipyridine)metal(II) bis(hexafluorophosphate), **1**(M = Ru, Os), exists in two diastereomeric forms. The crystal structures of the major diastereomers, (Δ,δ/Λ,λ)-**1**(M = Ru) and (Δ,δ/Λ,λ)-**1**(M = Os), have been determined. The 1,1′-biisoquinoline ligand is nonplanar, which is a result of a transannular steric interaction between H_8 and $H_{8'}$. The conformation of the five-membered chelate ring formed by the 1,1′-biisoquinoline ligand in the solid-state is λ when the configuration at the metal is Λ. As expected due to the lanthanide contraction effect, the molecular structure of **1**(M = Os) is comparable with the analogue **1**(M = Ru) with statistically-equivalent M−N bond distances. Diastereoisomerization of **1**(M = Ru, Os) in solution is facile. Spin perturbation NMR experiments demonstrate that the interconversion of the two diastereomers of **1**(M = Ru) and **1**(M = Os) is the result of an intramolecular process of C_2 symmetry that does not change the *cis/trans* relationship between the 1,1′-biisoquinoline and 2,2′-bipyridine ligands. The results of the earlier, more extensive study of **1**(M = Ru) and the present study of **1**(M = Os) are consistent with a mechanism for interconversion of the two diastereoisomers of **1** that involves atropisomerization of the η^2-1,1′-biisoquinoline ligand via a *syn* planar transition state. The rate of interconversion of **1**(M = Os) is an order of magnitude faster than the rate of interconversion of **1**(M = Ru): e.g., at 50 °C for **1**(M = Ru) $K = 2.71$ and $k(6a_{maj} \rightarrow 6a_{min}) = 1.43(6)\ s^{-1}$ and for **1**(M = Os) $K = 3.19$ and $k(6a_{maj} \rightarrow 6a_{min}) = 10.6(3)\ s^{-1}$. The free energy of activation for **1**(M = Ru) ($\Delta G_{50}^{\ddagger}$(maj → min) = 79(2) kJ mol^{-1}, $\Delta G_{50}^{\ddagger}$(min → maj) = 76(2) kJ mol^{-1}) is greater than the free energy of activation for **1**(M = Os) ($\Delta G_{50}^{\ddagger}$(maj → min) = 72(2) kJ mol^{-1}, $\Delta G_{50}^{\ddagger}$(min → maj) = 68(2) kJ mol^{-1}) in both the maj → min and min → maj directions. Based on the premise that metal−ligand bond strengths increase down a triad of transition metals, these kinetic and thermodynamic data support our hypothesis that the misdirected 1,1′-biisoquinoline ligand (bent M-N bonds) is redirected (optimally oriented M−N bonds) in the *syn* planar transition state. Thus, the metal that forms thermodynamically stronger M−N bonds (osmium) is more kinetically labile with respect to atropisomerization of the 1,1′-biisoquinoline ligand.

Introduction

The second law of thermodynamics tells us that a closed system will approach an equilibrium state. Thus given the thermodynamic parameters and the equations of state, we can predict with accuracy the position of an equilibrium.[1] However, thermodynamics is unable to predict the time required to achieve equilibrium. Nonetheless, the thermochemical properties of chemical substances place significant quantitative constraints on the kinetic parameters that describe a system at equilibrium.[2] The reason for this is that a true state of equilibrium is a dynamic state in which chemical changes are still taking place, albeit with equal forward and reverse rates. There has been considerable effort to relate the ground state structures of molecules (described by thermochemical parameters) with the transition state structures of reacting molecules (described by activation parameters). Such analyses yield "free energy relationships".[3] Substituent effects in such relationships can yield insight into the mechanisms of reactions, and of particular interest are systems that exhibit inverse thermodynamic stability/reactivity relationships whereby the thermodynamically more stable derivatives are kinetically more labile.[4] The present study examines the effect of perturbing the transition metal−ligand bond strength of a system with "misdirected" (bent) metal-ligand bonds that are "redirected" (optimally oriented) during an isomerization reaction. Thus, the relatively weak metal−ligand bonds in the ground state are strengthened in the transition state.

† Dedicated to Professor Jack Halpern on the occasion of his 70th birthday.

® Abstract published in *Advance ACS Abstracts,* February 1, 1995.

(1) Blandamer, M. J. *Chemical Equilibria in Solution*; Ellis Horwood and Prentice Hall: New York, 1992.

(2) Benson, S. W. *Thermochemical Kinetics*, 2nd ed.; Wiley-Interscience: New York, 1976.

(3) For reviews, see: (a) Topsom, R. D. *Prog. Phys. Org. Chem.* **1976**, *12*, 1. (b) Unger, S. H.; Hansch, C. *Prog. Phys. Org. Chem.* **1976**, *12*, 91. (c) Levitt, L. S.; Widing, H. F. *Prog. Phys. Org. Chem.* **1976**, *12*, 119. (d) Hine, J. *Structural Effects on Equilibria in Organic Chemistry*; Wiley: New York, 1975. (e) Ehrenson, S.; Brownlee, R. T. C.; Taft, R. W. *Prog. Phys. Org. Chem.* **1973**, *10*, 1. (f) Charton, M. *Prog. Phys. Org. Chem.* **1973**, *10*, 81. (g) Johnson, K. F. *The Hammett Equation*; Cambridge University Press: New York, 1973. (h) Godfrey, M. *Tetrahedron Lett.* **1972**, 753. (i) Exner, O. In *Advances in Linear Free Energy Relationships*; Chapman, N. B., Shorter, J. Eds.; Plenum Press: London, 1972; p 72. (j) Shorter, J. *Q. Rev. Chem. Soc.* **1970**, *24*, 433. (k) Wells, P. R. *Linear Free Energy Relationships*; Academic Press: New York, 1968. (l) Hammett, L. P. *Physical Organic Chemistry*, 2nd ed.; McGraw-Hill: New York, 1970; p 347. (m) Ritchie, C. D.; Sager, W. F. *Prog. Phys. Org. Chem.* **1964**, *2*, 323. (n) Ehrenson, S. *Prog. Phys. Org. Chem.* **1964**, *2*, 195. (o) Leffler, J. E.; Grunwald, E. *Rates and Equilibria of Organic Reactions*; Wiley: New York, 1963. (p) Hammett, L. P. *J. Am. Chem. Soc.* **1937**, *59*, 96.

(4) Pross, A. *Adv. Phys. Org. Chem.* **1977**, *14*, 69.

0002-7863/95/1517-2000$09.00/0

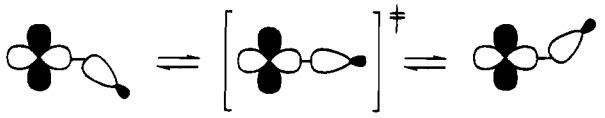

Perturbation of the metal−ligand bond strength of such a system is expected to reveal an inverse relationship between thermodynamic and kinetic stability. Accordingly, the derivatives with inherently stronger latent metal−ligand bonds might be expected to be more labile with respect to redirection of the misdirected ligand.

In contrast to the preferential planarity of most 2,2′-bipyridine ligands, the ligand 1,1′-biisoquinoline is expected to be nonplanar because of an unfavorable transannular steric interaction between H_8 and $H_{8'}$. Consequently, the metal complex Δ/Λ-(δ/λ-1,1′-biisoquinoline)bis(2,2′-bipyridine)ruthenium(II), **1**(M = Ru), is chiral at the metal center and the 1,1′-biisoquinoline ligand and therefore it exists in two diastereomeric forms.

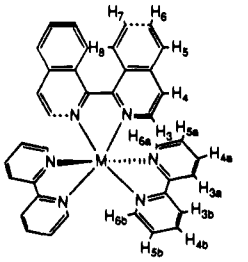

1 = $[M^{II}(bipy)_2(1,1'\text{-biiq})]^{2+}$ (M = Ru, Os)

We have established in a recent mechanistic study that interconversion of the two stereochemically labile diastereomers of **1**(M = Ru) takes place by a regular mechanism (without breaking Ru−N bonds) that involves atropisomerization of the η^2-1,1′-biisoquinoline ligand via a *syn* planar transition state.[5] Accordingly, the misdirected 1,1′-biisoquinoline ligand in the ground state structure of **1**(M = Ru) is redirected in the transition state that relates the two diastereomers of **1**(M = Ru).

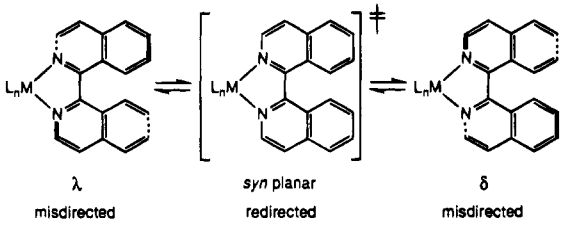

We report here the kinetics and mechanism of diastereoisomerization of the osmium derivative. The derivative **1**(M = Os) was chosen for this study because the geometries of **1**(M = Ru) and **1**(M = Os) are expected to be nearly identical (as a result of the lanthanide contraction effect), but the metal−ligand bond strengths should be markedly different. Crystal structure analyses demonstrate the two derivatives are isostructural with statistically equivalent bond distances and angles. Furthermore, we have learned that the mechanism of isomerization of **1**(M = Os) is the same as that previously reported for **1**(M = Ru). Although the steric factors that contribute to the barrier of atropisomerization of **1**(M = Ru) and **1**(M = Os) are presumably similar, we show herein that varying the metal−biisoquinoline bond strength has a marked influence on the kinetics of atropisomerization of the complexes; the rate of diastereoisomerization of **1**(M = Os) is an order of magnitude faster than the rate of diastereoisomerization of **1**(M = Ru). Based on the premise that metal-ligand bond strengths increase down a triad of transition metals,[6] a trend for which we are aware of no exceptions, the kinetic and thermodynamic data that are reported herein further supports our hypothesis that the misdirected 1,1′-biisoquinoline ligand is redirected in the *syn* planar transition state. Thus, the metal that forms stronger M−N bonds (osmium) is more labile with respect to redirection of the misdirected 1,1′-biisoquinoline ligand. To our knowledge, this represents the first report of a stronger bond being more reactive in a thermodynamically controlled (equilibrium) reaction.

Experimental Section

Materials. $(NH_4)_3OsCl_6$, NH_4PF_6, and 2,2′-bipyridine were used as received from Aldrich. $Os(bipy)_2Cl_2$[7] and 1,1′-biisoquinoline[5b] were prepared according to literature procedures. Reagent grade ethylene glycol, toluene, acetonitrile, pentane, ethyl ether, dichloromethane, and acetone-d_6 were used without further purifications.

Synthesis of (Δ,δ/Λ,λ)-1(M = Os) (Major) Diastereomer. $Os(bipy)_2Cl_2$ (100 mg, 0.17 mmol), 1,1′-biisoquinoline (100 mg, 0.39 mmol), and 20 mL of ethylene glycol were placed in a tube fitted with a high-pressure Teflon stopcock. The solution was freeze−pumped−thawed and left under vacuum, and the flask was placed in an 190 °C oil bath for 18 h. The remaining operations were carried out in the air. The purple solution was cooled to room temperature and an aqueous solution of NH_4PF_6 (1 g in 20 mL of water) was added to give a voluminous precipitate, which was collected by filtration, washed with water (5 × 10 mL) and ethyl ether (5 × 10 mL), and dried under vacuum. The solid was dissolved in a minimum amount of 1:1 toluene/acetonitrile and chromatographed on grade I neutral alumina (2.5 cm × 50 cm) eluting with 1:1 toluene/acetonitrile to give a purple band followed by a brown band. The purple band was collected as a single fraction, and the volatiles were removed with a rotary evaporator. The acetonitrile/toluene azeotrope (bp 81.1 °C) evaporated first leaving ca. 20 mL of toluene in which the product was suspended as a solid. The precipitate was removed by filtration, washed with toluene (5 × 10 mL) and pentane (5 × 10 mL), and dried under vacuum to give the product as a deep purple microcrystaline solid (143 mg, 78% based on $Os(bipy)_2Cl_2$). Anal. Calcd for $C_{38}H_{28}F_{12}N_6P_2Os$: C, 43.32; H, 2.69; N, 8.01. Found: C, 43.77; H, 2.84; N, 8.18.

Assignment of ^{1}H NMR Spectrum of 1(M = Os). Scalar coupling relationships between the protons were obtained using ^{1}H−^{1}H double-quantum-filtered homonuclear correlation spectroscopy (dqf-COSY)[8] at −80 °C, conditions under which chemical exchange is slow. (Δ,δ/Λ,λ)-1(M = Os) (major) diastereomer: ^{1}H NMR (acetone-d_6, 25 °C, 500 MHz) δ 8.85 (d, bipy-H_{3b}, J = 8.0 Hz); 8.77 (d, bipy-H_{3a}, J = 8.0 Hz); 8.40 (d, bipy-H_{6a}, J = 6.0 Hz); 8.25 (d, biiq-H_5, J = 8.0 Hz); 8.12 (d, biiq-H_8, J = 8.0 Hz); 8.05 (dt, bipy-H_{4b}, J = 6.0, 8.0 Hz); 7.96 (dt, bipy-H_{4a}, J = 6.0, 8.0 Hz); 7.94 (t, bipy-H_{6b}, J = 6.0 Hz); 7.90, 7.85 (d, biiq-$H_{3,4}$, J = 6.0 Hz); 7.81 (t, biiq-H_7, J = 8.0 Hz); 7.73 (t, biiq-H_6, J = 8.0 Hz); 7.54 (dt, bipy-H_{5b}, J = 6.0, 8.0 Hz); 7.31 (dt, bipy-H_{5a}, J = 6.0, 8.0 Hz). Complete assignment of the ^{1}H resonances of the minor diastereomer (Δ,λ/Λ,δ)-1(M = Os) was not possible since the 2,2′-bipy-d_8 analogue was not synthesized as in the case of **1**(M = Ru). Assignment of the ^{1}H spectrum of the minor diastereomer (Δ,λ/Λ,δ)-**1**(M = Os) was made even more difficult because the equilibrium constant for **1**(M = Os) is larger than that observed for **1**(M = Ru). However, the resonance that corresponds to bipy-H_{6a} was easily identified because it is well-resolved and shifted

(5) (a) Ashby, M. T.; Govindan, G. N.; Grafton, A. K. *Inorg. Chem.* **1993**, *32*, 3803. (b) Ashby, M. T.; Govindan, G. N.; Grafton, A. K. *J. Am. Chem. Soc.* **1994**, *116*, 4801.

(6) For a review of experimental data, see: Martinho Simões, J. A.; Beauchamp, J. L. *Chem. Rev.* **1990**, *90*, 629−699. For a discussion of theory, see: Ohanessian, G.; Goddard, W. A., III *Acc. Chem. Res.* **1990**, *23*, 386−392.

(7) Kober, E. M.; Caspar, J. V.; Sullivan, B. P.; Meyer, T. J. *Inorg. Chem.* **1988**, *27*, 4587.

(8) Rance, M.; Sorensen, O. W.; Bodenhausen, G.; Wagner, G.; Ernst, R. R.; Wüthrich, K. *Biochem. Biophys. Res. Commun.* **1983**, *117*, 479.

Table 1. Crystallographic Data for $(\Delta,\delta/\Lambda,\lambda)$-**1**(M = Os) at 25 °C[a]

formula	$C_{38}H_{28}F_{12}N_6P_2Os$
fw	1048.8
space group	*C*2/c (no. 15)
cell dimension[b]	
a, Å	29.094(9)
b, Å	18.61(1)
c, Å	17.855(9)
β, deg	127.93(3)
V, Å^3	7625(7)
Z	8
d_{calcd}, g cm^{-3}	1.83
crystal shape	rectangular prism
crystal dimensions, mm	0.40 × 0.32 × 0.26
radiation	Mo Kα (λ = 0.710 73 Å)[c]
absorption coefficient, mm^{-1}	0.468
data collection range, deg	3−45
no. of unique data	4982
no. of data used ($I > 2\sigma(I)$)	2908
R	0.027
R_w	0.037
GOF	4.92
largest shift/esd, final cycle	0.41

[a] The standard deviation of the least significant figure is given in parentheses in this and subsequent tables. $R = \sum||F_o| - |F_c||/\sum|F_o|$, $R_w = [\sum\omega(|F_o| - |F_c|)^2/\sum\omega|F_o|^2]^{1/2}$, GOF = $[\sum(\omega(|F_o| - |F_c|)^2/(m - n)]^{1/2}$. [b] The cell dimensions were obtained from a least-squares refinement of the setting angles of 25 reflections. [c] Monochromatized by a graphite crystal.

far up field as it is in $(\Delta,\lambda/\Lambda,\delta)$-**1**(M = Ru). Since the 2D EXSY spectrum indicates the same mechanism of diastereoisomerization is operating for **1**(M = Os) as was previously described for **1**(M = Ru), this is the only resonance that is necessary to carry out the kinetic measurements of this study (*vide infra*). $(\Delta,\lambda/\Lambda,\delta)$-**1**(M = Os) (minor) diastereomer: ^{1}H NMR (acetone-d_6, 25 °C, 500 MHz): δ 7.13 (d, bipy-H_{6a}, J = 6.0 Hz).

NMR Studies. Single crystals of **1**(M = Os) were dissolved in acetone-d_6 to give 10−20 mM solutions. The solutions were transferred to 5 mm NMR tubes that had been glass-blown onto vacuum-line adaptors fitted with high-vacuum Teflon stopcocks. The samples were put through two freeze−pump−thaw cycles, left under vacuum, and then flame sealed while the solutions were still frozen. Spin inversion transfer (SIT)[9] and two dimensional exchange spectroscopy (2D EXSY)[10] were carried out on a Varian VXR-500 NMR spectrometer as described previously for **1**(M = Ru).[5b] A comparison between the kinetic and thermodynamic data that were previously obtained for **1**(M = Ru) and those data for **1**(M = Os) that were measured in the present study is given in Tables 5 and 6.

X-ray Diffraction Study of $(\Delta,\delta/\Lambda,\lambda)$-1(M = Os). X-ray data were collected with an Enraf-Nonius CAD4 diffractometer using monochromated Mo Kα radiation (λ = 0.710 69 Å) and methods standard in this laboratory.[11] The crystallographic data are summarized in Table 1. Automatic centering, indexing, and least-squares routines were used to obtain the cell dimensions. The data were collected and corrected for Lorentz and polarization effects;[12] however, no absorption correction was applied since it was judged to be negligible. Crystal integrity was followed by periodically recollecting three monitor reflections. No decay was observed. The structures were solved by direct methods using the SHELX-86[13] program. Refinement of the structures was by block-matrix least-squares calculations using SHELX-76[14] initially with isotropic and finally with anisotropic temperature factors for the non-hydrogen atoms. Neutral scattering factors were used for all atoms.[15] A difference map at an intermediate stage of refinement revealed maxima consistent with the positions of hydrogen atoms which were included in the subsequent cycles of refinement in idealized positions with isotropic temperature factors that reflected the temperature factors of the aromatic carbon atoms to which they are bound. Unit weights were used in the early stages of refinement and weights derived from counting statistics were used in the final cycles of refinement. A difference map calculated at the end of the refinement showed no chemically significant features. ORTEP views of (Λ,λ)-**1**(M = Os) are given in Figures 1 and 2. Comparisons of selected interatomic distances, interatomic angles, and torsion angles for $(\Delta,\delta/\Lambda,\lambda)$-**1**(M = Ru) and $(\Delta,\delta/\Lambda,\lambda)$-**1**(M = Os) are presented in Tables 2−4. Other data are available as supplementary material.

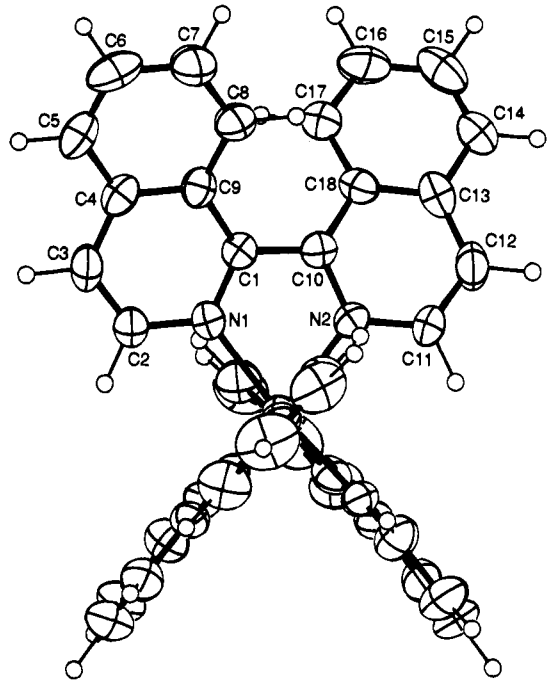

Figure 1. ORTEP drawing of (Λ,λ)-**1**(M = Os) showing the labeling scheme of the 1,1′-biisoquinoline ligand. Atoms are represented by thermal vibration ellipsoids at the 50% level. Hydrogen atoms have been assigned arbitrary thermal parameters.

Results and Discussion

Solution and Solid-State Structures of 1(M = Os). The ^{1}H NMR spectrum of **1**(M = Os) in acetone solutions at 25 °C reveals an ~3:1 mixture of the two diastereomers. The specific relative configuration of **1**(M = Ru) in solution has been established[5] and the chemical shifts of **1**(M = Os) are similar. We therefore conclude that the major diastereomer of **1**(M = Os) has a λ conformation at the 1,1′-biisoquinoline ligand when the metal has a Λ configuration. A single-crystal X-ray structure determination of **1**(M = Os) was undertaken to obtain more information regarding its structure. The crystals of **1**(M = Os) were found to be isomorphous with those that were previously studied for **1**(M = Ru), thus the crystal structure is of the $(\Delta,\delta/\Lambda,\lambda)$-**1**(M = Os) (major) diastereoisomer, as demonstrated by the successful refinement of the structure. Comparisons of selected structural data for $(\Delta,\delta/\Lambda,\lambda)$-**1**(M = Ru) and $(\Delta,\delta/\Lambda,\lambda)$--**1**(M = Os) are given in Tables 2−4. These data clearly demonstrate that the structures are similar. In particular, most

(9) (a) Alger, J. R.; Prestegard, J. H. *J. Magn. Reson.* **1977**, *27*, 137. (b) Kuchel, R. W.; Chapman, B. E. *J. Theor. Biol.* **1983**, *105*, 569. (c) Robinson, G.; Kuchel, P. W.; Chapman, B. E. *J. Magn. Reson.* **1985**, *63*, 314. (d) Bellon, S. F.; Chen, D.; Johnston,E. R. *J. Magn. Reson.* **1987**, *73*, 168.

(10) Abel, E. W.; Coston, T. P. J.; Orrell, K. G.; Sik, V.; Stephenson, D. *J. Magn. Reson.* **1986**, *70*, 34.

(11) (a) Khan, M. A.; Taylor, R. W.; Lehn, J. M.; Dietrich, B. *Acta Crystallogr.* **1988**, *C44*, 1928. (b) Ashby, M. T.; Khan, M. A.; Halpern, J. *Organometallics* **1991**, *10*, 2011.

(12) Walker, N.; Stuart, D. *Acta Crystallogr.* **1983**, *A39*, 158.

(13) Sheldrick, G. M. *Crystallographic Computing 3*; Sheldrick, G. M.; Kruger, C.; Goddard, R., Eds.; Oxford University Press: Oxford, England, 1985; pp 175−189.

(14) Sheldrick, G. M. *SHELX-76. A Program for Crystal Structure Determination*; University of Chambridge: Chambridge, England, 1976.

(15) International Tables for X-ray Crystallography, Kynoch Press: Birmingham, England, 1974; Vol. IV, pp 99, 149.

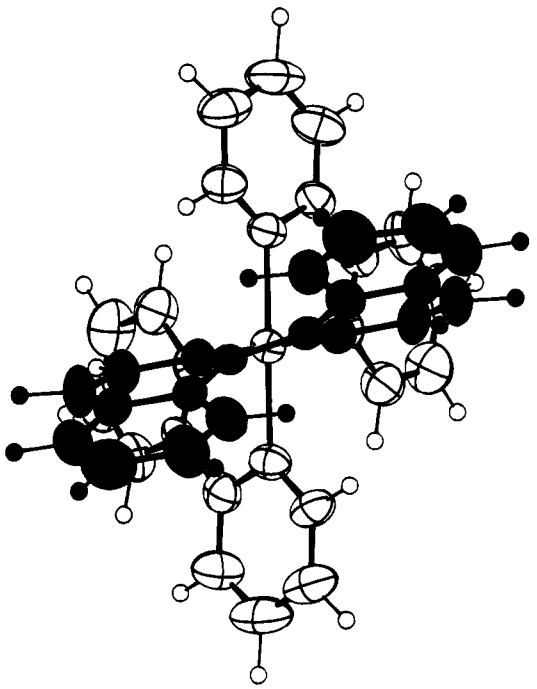

Figure 2. Top-down ORTEP drawing of (Λ,λ)-**1**(M = Os). Atoms are represented by thermal vibration ellipsoids at the 50% level. Hydrogen atoms have been assigned arbitrary thermal parameters.

Table 2. Comparison of Selected Interatomic Distances (Å) for the Ru and Os Derivatives of (Δ,δ/Λ,λ)-**1**

	M = Ru	M = Os
M−N1	2.061(4)	2.049(7)
M−N2	2.062(4)	2.043(7)
M−N3	2.053(4)	2.064(7)
M−N4	2.063(4)	2.074(7)
M−N5	2.070(4)	2.071(7)
M−N6	2.048(4)	2.071(6)

Table 3. Comparison of Selected Interatomic Angles (deg) for the Ru and Os Derivatives of (Δ,δ/Λ,λ)-1[a]

	M = Ru	M = Os
N1−M−N2	77.90(18)	76.9(3)
N1−M−N3	97.41(17)	98.0(3)
N1−M−N4	174.74(16)	174.2(3)
N1−M−N5	97.80(18)	97.9(3)
N1−M−N6	88.77(16)	88.1(3)
N2−M−N3	88.44(16)	88.4(3)
N2−M−N4	97.80(18)	98.8(3)
N2−M−N5	174.81(15)	174.1(3)
N2−M−N6	97.67(16)	98.4(3)
N3−M−N4	79.32(17)	78.0(3)
N3−M−N5	95.05(17)	95.0(3)
N3−M−N6	172.12(15)	171.8(3)
N4−M−N5	86.65(17)	86.6(3)
N4−M−N6	94.86(17)	96.4(3)
N5−M−N6	79.21(17)	78.6(3)
L1−M−L2	121.11(3)	121.2(1)
L2−M−L3	117.51(1)	122.1(1)
L1−M−L3	121.37(3)	113.3(1)

[a] L1 is the midpoint between the σ bond of the 1,1′-biisoquinoline ligand. L2 and L3 are the midpoints between the σ bonds of the 2,2′-bipyridine ligands.

of the corresponding bond distances and angles are identical within experimental error (using the accepted criterion of three estimated standard deviations). This is consistent with the lanthanide contraction effect.[16] However, we note that the N1−C1−C10−N2 torsion angle that describes the twist of the 1,1′-biisoquinoline ligand is significantly more acute in the case of (Δ,δ/Λ,λ)-**1**(M = Os) as compared with (Δ,δ/Λ,λ)-**1**(M = Ru). This may reflect a greater effort to redirect the misdirected 1,1′-biisoquinoline ligand in the osmium derivative (*vide infra*).

(16) Lloyd, D. R. *J. Chem. Educ.* **1986**, *53*, 502.

Table 4. Comparison of Selected Torsion Angles (deg) for the Ru and Os Derivatives of Λ(λ)-**1**

	M = Ru	M = Os
N1−C1−C10−N2	−24.1(6)	−20.1(10)
N3−C19−C24−N4	−3.4(8)	−4.8(13)
N5−C29−C34−N6	−3.0(8)	−2.9(13)

Mechanism of Diastereoisomerization of 1(M = Os). Because chemical exchange is slow on the NMR time scale, a discrete, static room temperature spectrum is obtained for the two diastereomers of **1**(M = Os). Significant line broadening is observed at 500 MHz as the dynamic diastereoisomerization process becomes fast on the NMR time scale at temperatures above ~50 °C. Since the chemical exchange is fast with respect to spin−lattice relaxation above temperatures of ~20 °C, spin perturbation/recovery techniques may be used to probe the kinetics of isomerization in the temperature range of 20−50 °C. The three NMR methods that are generally employed to investigate dynamic phenomenon that are slow on the NMR time scale but are fast with respect to spin relaxation are spin saturation transfer (SST),[17] spin inversion transfer (SIT),[18] and two dimensional exchange spectroscopy (2D EXSY).[19] We employed 2D EXSY to investigate the symmetry of chemical exchange. A complete assignment of the ^{1}H NMR spectrum of **1** is necessary to interpret the results of the 2D EXSY experiment. In particular, it is necessary to assign the resonances that correspond to the symmetry inequivalent halves of the 2,2′-bipyridine ligands. Fortunately, this proved possible for both diastereoisomers of **1**(M = Ru). Although it was possible to assign the ^{1}H NMR spectrum of the major diastereomer (Δ,δ/Λ,λ)-**1**(M = Os), it was not possible to completely assign the spectrum of the minor diastereomer (Δ,λ/Λ,δ)-**1**(M = Os). However, because of our previous success in assigning the spectrum of **1**(M = Ru) and the similarity of the 2D EXSY spectra that were obtained for **1**(M = Ru) (published previously)[5] and **1**(M = Os) (Figure 3), we conclude that the mechanism of diastereoisomerization of **1**(M = Os) is similar to that previously described for **1**(M = Ru); the C_2 symmetry and *cis*/*trans* relationship of the 2,2′-bipyridine ligands are maintained during the interconversion of the diastereomers of **1**. Note in particular the cross peak that corresponds to chemical exchange between H_{6a}(major) at 8.40 ppm and H_{6a}(minor) at 7.13 ppm. Thus we conclude that the mechanism involves atropisomerization of the η^2-1,1′-biisoquinoline ligand via a *syn* planar transition state.

Kinetics and Thermodynamics of Atropisomerization of 1(M = Os). Having concluded from the 2D EXSY experiment that the mechanism for diastereoisomerization of **1**(M = Os) is similar to that previously discussed for **1**(M = Ru), we carried out an investigation of the kinetics of the atropisomerization of **1**(M = Os). Complete assignment of the ^{1}H NMR spectra of **1**(M = Os) is in fact unnecessary to carry out these kinetic studies. It is necessary to identify unambiguously only one resonance of each diastereomer that is undergoing chemical

(17) (a) Faller, J. W. *Adv. Organomet. Chem.* **1977**, *16*, 211. (b) Green, M. L. H.; Sella, A.; Wong, L.-L. *Organometallics* **1992**, *11*, 2650.

(18) (a) Alger, J. R.; Prestegard, J. H. *J. Magn. Reson.* **1977**, *27*, 137. (b) Kuchel, R. W.; Chapman, B. E. *J. Theor. Biol.* **1983**, *105*, 569. (c) Robinson, G.; Kuchel, P. W.; Chapman, B. E. *J. Magn. Reson.* **1985**, *63*, 314. (d) Bellon, S. F.; Chen, D.; Johnston,E. R. *J. Magn. Reson.* **1987**, *73*, 168.

(19) Abel, E. W.; Coston, T. P. J.; Orrell, K. G.; Sik, V.; Stephenson, D. *J. Magn. Reson.* **1986**, *70*, 34.

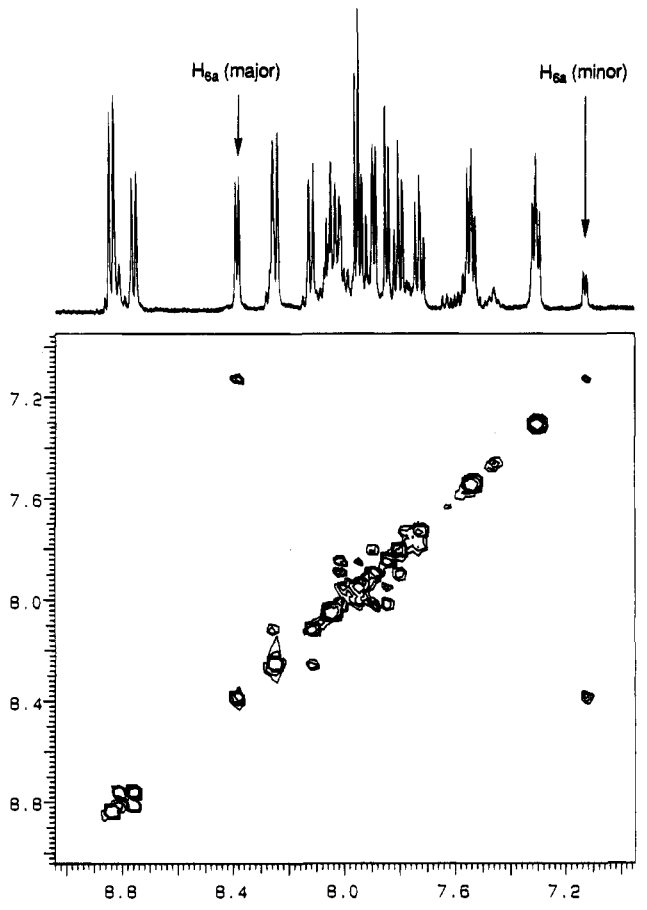

Figure 3. 2D EXSY spectrum at 500 MHz and 50 °C revealing the interconversion of (Δ,δ/Λ,λ)-**1**(M = Os) and (Δ,λ/Λ,δ)-**1**(M = Os).

Table 5. Comparison of the Kinetic Data Obtained for the Diastereoisomerization of the Ru and Os Derivatives of (Δ,δ/Λ,λ)-**1**[a]

	M = Ru		M = Os	
T (°C)	K[b]	k_1 (s^{-1})	K[b]	k_1 (s^{-1})
20	*c*	*d*	3.58	0.81(6)
30	*c*	*d*	3.40	1.86(9)
40	*c*	*d*	3.29	4.7(1)
50	2.71	1.43(6)	3.19	10.6(3)
60	2.76	3.3(1)	*e*	*e*
70	2.86	6.9(2)	*e*	*e*
80	2.88	12.7(3)	*e*	*e*
90	3.04	27(2)	*e*	*e*

[a] The rate data were measured by irradiating bipy-H_{6a} (maj) and observing bipy-H_{6a} (min). This yields the rate constant for the major diastereomer isomerizing to the minor diastereomer. [b] The equilibrium constants K = [maj]/[min] were measured by integration of the ^{1}H NMR spectra and are accurate to approximately ±3%. [c] Not measured. [d] The rate of exchange becomes slower than the rate of spin relaxation of bipy-H_{6a} (maj). [e] The spectrum becomes dynamic as the rate of exchange becomes fast on the NMR time scale.

exchange. Since the mechanism involves the pairwise exchange of nuclei, the more accurate SIT method could be utilized in this study (rather than SST). The resonances that correspond to H_{6a} of the major and minor isomers were respectively irradiated and observed in the SIT experiments. The kinetic data from the earlier study of **1**(M = Ru) and the data of the present study of **1**(M = Os) are summarized in Table 5. The rates observed for **1**(M = Os) are substantially faster that those that were observed for **1**(M = Ru) under similar conditions, as reflected in the rate constants that are listed in Table 5 (e.g., at 50 °C for **1**(M = Ru) K = 2.71 and $k(6a_{maj} \rightarrow 6a_{min})$ = 1.43(6) s^{-1} and for 1(M = Os) K = 3.19 and $k(6a_{maj} \rightarrow 6a_{min})$ = 10.6(3) s^{-1}). The activation parameters are summarized in Table 6. The free energy of activation for **1**(M = Ru) ($\Delta G_{50}^{\ddagger}$(maj → min) = 79(2) kJ mol^{-1}, $\Delta G_{50}^{\ddagger}$(min → maj) = 76(2) kJ mol^{-1}) is greater than the free energy of activation for **1**(M = Os) ($\Delta G_{50}^{\ddagger}$(maj → min) = 72(2) kJ mol^{-1}, $\Delta G_{50}^{\ddagger}$(min → maj) = 68(2) kJ mol^{-1}) in both the maj → min and min → maj directions. We note that the enthalpies and entropies of activation of the two derivatives do not appear to be consistent between the ruthenium and osmium derivatives (e.g., for **1**(M = Ru) $\Delta H^{\ddagger}$(min → maj) > $\Delta H^{\ddagger}$(maj → min), but for **1**(M = Os) $\Delta H^{\ddagger}$(maj → min) > $\Delta H^{\ddagger}$(min → maj)); however, the estimated standard errors associated with these numbers and the narrow temperature ranges that were investigated[20] tend to invalidate such comparisons.

Free Energy Relationship between the Kinetic Stabilities of 1. We have previously noted[5b] that in its ground state structure the σ-donor orbitals of the twisted 1,1′-biisoquinoline ligand are misdirected with respect to the σ-acceptor orbitals of the metal.[21] A *syn* planar 1,1′-biisoquinoline ligand would direct the ligand's σ-donor orbitals toward the metal's σ-acceptor orbitals,[22] which could help overcome the energy required to distort the 1,1′-biisoquinoline ligand sufficiently to allow H_8 and $H_{8'}$ to pass by one another. In this regard strengthening the metal−ligand bonds may actually facilitate the atropisomerization reaction. The osmium derivative of **1** was selected for comparison to the ruthenium derivative that was previously studied because third row transition metal−ligand bonds are stronger than second row transition metal−ligand bonds,[23] a trend that is attributed to a corresponding increase in metal−ligand orbital overlap down a triad.[24] It seems reasonable that strengthening the metal−ligand bonds (e.g., by changing the metal) should have a greater effect on the transition state where the donor orbitals of the 1,1′-biisoquinoline ligand are more optimally directed toward the metal's acceptor orbitals as compared with the ground state orientation in which the donor orbitals of the 1,1′-biisoquinoline ligand are misdirected. The effect of perturbing the metal−ligand bond strength on the barrier to atropisomerization of the 1,1′-biisoquinoline ligand of **1** may be visualized by conceptually dividing the energetic barrier into steric and electronic components (Figure 4), the steric component being associated with the steric (and electronic) factors that are associated with atropisomerization of the "free" ligand via a *syn* planar transition state and the electronic component being associated with the inherent modification of the metal−biisoquinoline bonds during the atropisomerization reaction. First, the kinetic barrier to atropisomerization can be

(20) For an example of combining NMR kinetic data in the "fast-exchange" and "slow-exchange" regimes to extend the temperature range studied and improve the accuracy of the activation parameters, see: McAteer, C. H.; Moore, P. *J. Chem. Soc., Dalton Trans.* **1983**, 353.

(21) Ashby, M. T.; Lichtenberger, D. L. *Inorg. Chem.* **1985**, *24*, 636.

(22) Ashby, M. T.; Enemark, J. H.; Lichtenberger, D. L.; Ortega, R. B. *Inorg. Chem.* **1986**, *25*, 3154.

(23) For trends in metal−hydride bond dissociation energies, see: Bauschlicher, C. W., Jr.; Langhoff, S. R. In *Transition Metal Hydrides*; Dediev, A., Ed.; VCH: New York, 1992. For trends in homoleptic group 4 metal−alkyl bond dissociation energies, see: Skinner, H. A. *J. Chem. Thermodyn.* **1978**, *10*, 314. For trends in homoleptic group 6 metal−carbonyl bond dissociation energies, see: Hoff, C. D. In *Prog. Inorg. Chem.* Lippard, S. J., Ed.; John Wiley: New York, 1992; Vol. 40, pp 519−520, and references therein. For trends in the dissociation energies of various heteroatom−donor ligands, see: Ziegler, T.; Tschinke, V. In *Bonding Energetics in Organometallic Compounds*; Marks, T. J., Ed.; American Chemical Society: Washington, DC, 1990; pp 279−292. For a comparison of 4d-4d and 5d-5d metal−metal bonds, see: Collman, J. P.; Garner, J. M.; Hembre, R. T.; Ha, Y. *J. Am. Chem. Soc.* **1992**, *114*, 1292. For a comparison of activation of methane by first-, second-, and third-row metals, see: Irikura, K. K.; Goddard, W. A., III *J. Am. Chem. Soc.* **1994**, *116*, 8733 and references therein.

(24) Ziegler, T.; Tschinke, V.; Versluis, L.; Baerends, E. J.; Ravenek, W. *Polyhedron* **1988**, *7*, 1625.

Table 6. Comparison of the Thermodynamic Data Obtained for the Atropisomerization of the Ru and Os Derivatives of (Δ,δ/Λ,λ)-**1**[a]

M	$\Delta H^{\ddagger}$(maj → min), kJ mol^{-1}	$\Delta S^{\ddagger}$(maj → min), J K^{-1} mol^{-1}	$\Delta H^{\ddagger}$(min → maj), kJ mol^{-1}	$\Delta S^{\ddagger}$(min → maj), J K^{-1} mol^{-1}	$\Delta G_{50}^{\ddagger}$(maj → min), kJ mol^{-1}	$\Delta G_{50}^{\ddagger}$(min → maj), kJ mol^{-1}	$\Delta G_{50}°$, kJ mol^{-1}
Ru	68(2)	−33(4)	70(2)	−17(5)	79(2)	76(2)	2.7
Os	66(2)	−24(5)	63(2)	−23(6)	72(2)	68(2)	3.1

[a] The enthalpies and entropies of activation were determined from Eyring plots. The Gibbs free energies of activation at 50 °C were calculated from the enthalpies and entropies of activation. Energies of activation that were calculated from Arhenius plots exhibited the same trends. The Gibbs free energies of reaction were calculated from the equilibrium constants at 50 °C.

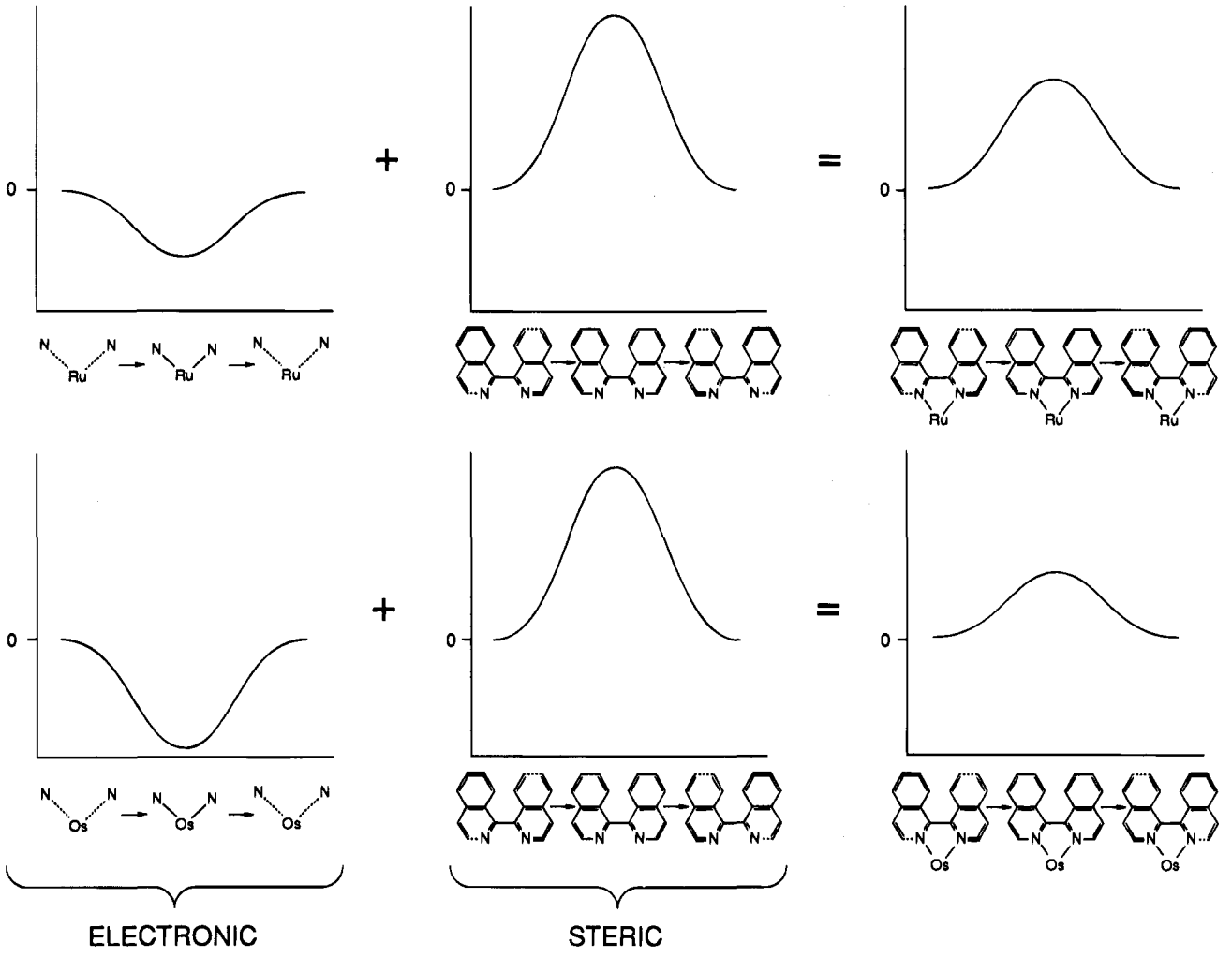

Figure 4. Conceptual partitioning of the electronic and steric effects associated with atropisomerization of two isomers of **1** with $K = 1$.

largely attributed to the energy that is required to distort the 1,1′-binaphthylene ring system of the ligand so as to permit the H_8 and $H_{8'}$ atoms to pass one another. This later, steric barrier is presumably the same for **1**(M = Ru) and **1**(M = Os) because of the similarity of their structures (Figure 4, middle). However, electronic factors should also contribute to the kinetic barrier of atropisomerization. We have suggested that the 1,1′-biisoquinoline ligand is misdirected in its ground-state orientation, but it is redirected in the transition state of atropisomerization. Accordingly, there should be a stabilization energy associated with redirection of the ligand. Such a stabilization energy should be greater for the osmium derivative as compared to the ruthenium derivative of **1** (Figure 4, left). Accordingly since we observe that the atropisomerization of **1**(M = Os) is facile with respect to **1**(M = Ru), the kinetic data reported herein support our earlier hypothesis that the M−N bonds of the 1,1′-biisoquinoline ligand are made stronger in the transition state of diastereoisomerization of **1** (Figure 4, right).

Rate−Equilibrium Relationship. There are two reasons to compare the equilibrium constants that reflect the relative stabilities of the diastereomers of **1**(M = Ru) and **1**(M = Os). First, unless the equilibrium constants of the two derivatives are very similar, one cannot simply compare the reaction rates as we have above. There is in fact a small, but statistically significant difference between the equilibrium constants (e.g., at 50 °C for **1**(M = Ru) $K = 2.71(8)$ and for **1**(M = Os) $K = 3.19(9)$), but this small difference cannot account for the order of magnitude difference in the rates of reaction of **1**(M = Ru) and **1**(M = Os) (e.g., at 50 °C for **1**(M = Ru) $k(6a_{maj} \rightarrow 6a_{min}) = 1.43(6)$ s^{-1} and for **1**(M = Os) $k(6a_{maj} \rightarrow 6a_{min}) = 10.6(3)$ s^{-1}). Accordingly, the barriers of atropisomerization are higher for the ruthenium derivative in both the maj → min and min → maj directions (e.g., for **1**(M = Ru) $\Delta G_{50}^{\ddagger}$(maj → min) = 79-(2) kJ mol^{-1} and $\Delta G_{50}^{\ddagger}$(min → maj) = 76(2) kJ mol^{-1} and for **1**(M = Os) $\Delta G_{50}^{\ddagger}$(maj → min) = 72(2) kJ mol^{-1} and $\Delta G_{50}^{\ddagger}$-(min → maj) = 68(2) kJ mol^{-1}). The second reason for considering the relative magnitudes of the equilibrium constants relates to the opening paragraph of this paper that reminds the reader that there is often a free energy relationship between equilibrium and rate constants. Indeed, this is the basis of the

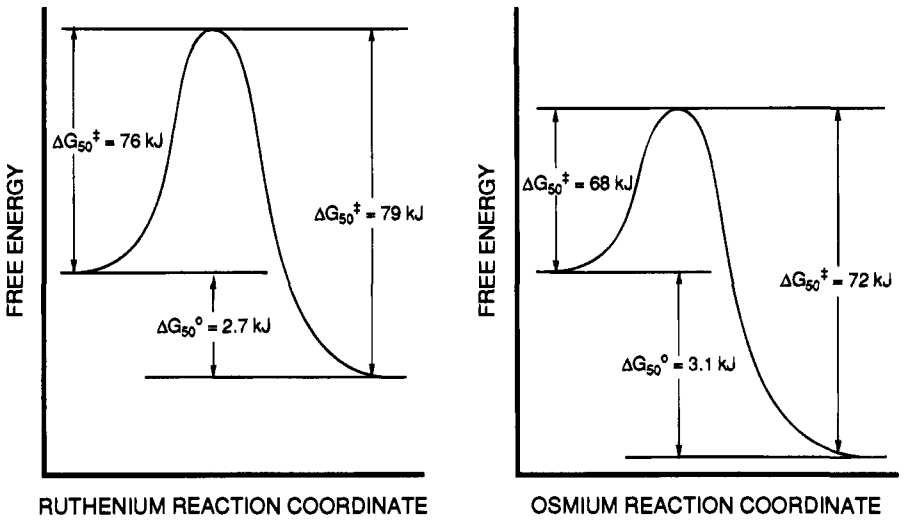

Figure 5. Reaction profiles for the atropisomerization of the major isomer ($\Delta,\delta/\Lambda,\lambda$)-**1**(M = Ru, Os) and minor isomer ($\Delta,\lambda/\Lambda,\delta$)-**1**(M = Ru, Os). The scales have been exaggerated to emphasize the differences between the reaction profiles of the two derivatives.

Hammett principle. At the risk of over interpreting the available data, it is useful in conclusion to consider the effect of the bonding considerations that were discussed above (misdirection and redirection) on the partitioning of the major and minor diastereoisomers of **1**.

The Hammett principle predicts that a parallelism should exist between reaction rates and equilibria (eq 1).[25]

$$\log \frac{k_1}{k_1^\circ} = \beta \log \frac{K}{K^\circ} \tag{1}$$

or

$$\delta \Delta G^\ddagger = \beta \, \delta \, \Delta G^\circ \tag{2}$$

If such an equation is valid, then a similar equation should exist for the reverse reaction (eq 3).

$$\log \frac{k_{-1}}{k_{-1}^\circ} = (1 - \beta) \log \frac{K}{K^\circ} \tag{3}$$

In terms of the present reaction, perturbation of the diastereoisomerization of **1** by substitution of the metal will simultaneously modify the energies of the major diastereomer (δG_{maj}°), the minor diastereomer (δG_{min}°), and the transition state ($\delta G^\ddagger$). If eq 1 holds, it may be rewritten as eq 4.

$$\delta G^\ddagger - \delta G_{maj}^\circ = \beta(\delta G_{min}^\circ - \delta G_{maj}^\circ) \tag{4}$$

Since the equilibrium constants of the present reactions are greater than unity, transition state theory[26] predicts that the transition states will be more like the minor diastereomers. Accordingly, $\delta G^\ddagger$ should be closer to δG_{min}° than to δG_{maj}°, and the constant β will approach unity as the equilibrium constant becomes larger. Given the latter expectation, the question arises is $\delta G_{maj}^\circ > \delta G_{min}^\circ$ or is $\delta G_{maj}^\circ < \delta G_{min}^\circ$? If the equilibrium is driven by electronic factors (i.e., M−N bond strength), the major diastereomer should exhibit stronger metal−biisoquinoline bonds; therefore, the M−N bonds of the major diastereomer should be affected to a greater extend by substitution of M and $\delta G_{maj}^\circ > \delta G_{min}^\circ$. If $\delta G_{maj}^\circ > \delta G_{min}^\circ$, $\delta G^\ddagger$ should be smaller for the derivative that bears stronger M−N bonds. Accordingly, the osmium derivative should not only be kinetically more labile with respect to atropisomerization, but it should also exhibit greater diastereoselectivity. This proves to be the case as reflected in the reaction profile of Figure 5.[27]

Thus in proceeding in the min → maj direction, atropisomerization of **1**(M = Os) is more exothermic than **1**(M = Ru) by $\delta\Delta G^\circ$ = 0.6 kJ mol^{-1} and the activation barrier is $\delta\Delta G^\ddagger$ = −5.7 kJ mol^{-1} less, yielding β = −9.5. Proceeding in the maj → min direction, atropisomerization of **1**(M = Os) is more endothermic than **1**(M = Ru) by $\delta\Delta G^\circ$ = −0.6 kJ mol^{-1} and the activation barrier is $\delta\Delta G^\ddagger$ = 5.1 kJ mol^{-1} more, yielding β = −8.5. The negative value for β can be understood in terms of the bonding considerations that have already been discussed, but the so-called anomalous values for β (i.e., $|\beta| > 1$) cannot be interpreted in terms of common theories.[28] Instead, the anomalous value of β can probably be attributed to the fact that the structures of the reactants and the products are similar; therefore, $\delta\Delta G^\circ$ differs only slightly and eqs 1 and 3 become invalid.[25]

Conclusions

An earlier detailed mechanistic study established that interconversion of the two diastereoisomers of **1**(M = Ru) takes place by a regular mechanism that involves atropisomerization of the η^2-1,1′-biisoquinoline ligand via a *syn* planar transition state.[5b] The results that are reported here for the osmium derivative **1**(M = Os) support a similar mechanism. We hypothesized following our earlier study that the misdirected donor orbitals of the twisted 1,1′-biisoquinoline ligand in the ground state of **1** are redirected in the transition state and that strengthening the transition metal−ligand bonds may actually facilitate the atropisomerization reaction.[5] The kinetic data for atropisomerization of **1** that are reported herein support this hypothesis; the osmium derivative with its presumed stronger

(25) Exner, O. *Correlation Analysis of Chemical Data*; Plenum Press: New York, 1988; pp 195−202.
(26) Albery, W. J. *Adv. Phys. Org. Chem.* **1993**, *28*, 139−170.

(27) There is an alternative and perhaps more simple way of viewing the relative magnitudes of the equilibrium constants. If the equilibrium constants are indeed determined by electronic factors, the effect of perturbation of M should be greatest for the major diastereomer with its stronger metal−biisoquinoline bonds. Thus, $\delta G_{maj}^\circ > \delta G_{min}^\circ$ and the equilibrium constant (in the maj → min direction) should become smaller the stronger the M−N bonds become. By way of analogy, for an equilibrium such as the H/D exchange reaction given below:

$$X{-}H + Y{-}D = X{-}D + Y{-}H$$

the heavier isotope (with its lower zero-point energy) will accumulate in the stronger bond in a thermodynamically-controlled (equilibrium) isotope exchange reaction.

(28) Lin, A. C.; Chiang, Y.; Dahlberg, D. B.; Kresge, A. J. *J. Am. Chem. Soc.* **1983**, *105*, 5380.

metal−ligand bonds is kinetically more labile as compared to the ruthenium derivative with respect to atropisomerization. Finally, we note that this trend in the thermodynamic stability/kinetic lability of **1** runs contrary to the usual situation in which thermodynamically more stable compounds tend to be kinetically more inert.[29] To our knowledge, this represents the first report of a stronger bond being more reactive in a thermodynamically controlled (equilibrium) reaction,[30] a trend that we attribute to redirection of the misdirected 1,1′-biisoquinoline ligand during atropisomerization.

Acknowledgment. The donors of the Petroleum Research Fund, administered by the ACS, are thanked for support of this research. The author is grateful to Prof. R. L. Halterman for reading the manuscript and providing valuable comments.

(29) The comparison that we are making here is one between relatively weak ruthenium bonds and relatively strong osmium bonds, not the relative stability of the minor and major diastereomer. Of course if ΔG° increases (the equilibrium constant increases) for a particular reaction, transition state theory predicts (and we observe) a decrease in $\Delta G^\ddagger$. This statement should not be confused with the so-called Marcus inverted region where a reaction becomes slower as it becomes more exothermic, see: Suppan, P. *Top. Curr. Chem.* **1992**, *163*, 95−130.

Supplementary Material Available: Tables of the crystallographic data, positional and thermal parameters of (Δ,δ/Λ,λ)-**1**(M = Os) (8 pages). This material is contained in many libraries on microfiche, immediately follows this article in the microfilm version of the journal, can be ordered from the ACS, and can be downloaded from the Internet; see any current masthead page for ordering information and Internet access instructions.

JA943538B

(30) There are, of course, many examples of kinetically controlled (irreversible) reactions that yield a thermodynamically unfavorable product. There are also examples of thermodynamically stronger bonds reacting faster in irreversible reactions. A good example of this would be a reaction that exhibits an inverse primary H/D isotope effect.[31] On thermodynamic grounds, breaking the X−D bond should be slower than breaking the X−H bond. However, if the bond formed is considerably stronger than the bond that is broken and the transition state is a late one, $\Delta G_D^\ddagger$ can be less than $\Delta G_H^\ddagger$, giving rise to an inverse primary H/D isotope effect $k_H/k_D < 1$. We are aware of a published report of a H/D exchange reaction that gives rise to an inverse primary isotope effect, a reaction that involves breaking a weak Mn−H bond and forming a strong C−H bond.[32]

(31) Leusink, A. J.; Budding, H. A.; Drenth, W. *J. Organomet. Chem.* **1967**, *9*, 295.

(32) Sweany, R. L.; Halpern, J. *J. Am. Chem. Soc.* **1977**, *99*, 8335.